Entry to the Stockholm Junior Water Prize 2015

Novel Renewable Filter for Heavy Metal Removal

A Practical Application of Functionalized Multi-Walled Carbon Nanotubes

Perry Alagappan

United States of America

I. SUMMARY

The objective of this project was to develop an effective, renewable filter to remove toxic heavy metal contaminants that permeate our water supplies due to the proliferation of electronic waste. Multi-Walled Carbon Nanotubes (MWNTs) were deposited on 3.45 g of Quartz Wool, purified through wet air oxidation and Hydrochloric acid sonification, and functionalized with epoxides to produce the filter medium. 0.052 M, 0.01 M, 0.01 M, 0.001 M, and 100 ppm solutions of Cadmium (II) Acetate, Mercuric Chloride, Nickel (II) Nitrate, Cobalt (II) Chloride, and Lead (II) Acetate respectively were poured into 0.5 g filter medium samples packed in a burette. A 50:50 solution of de-ionized water and acetic acid was used for renewal. Characterization techniques employed were: Ultraviolet-Visible Spectroscopy (UV-Vis) for filtration capacities, Scanning Electron Microscopy (SEM) for MWNT growth-patterns on quartz wool, Raman spectroscopy for changes in nanotube purity, and X-Ray Photoelectron Spectroscopy (XPS) for filter composition after filtration and renewal. UV-Vis revealed 3-trial average filtration capacities of 99.39%, 99.61%, 99.70%, 99.72%, and 99.97% for Cadmium, Mercury, Nickel, Cobalt, and Lead respectively. Progression of Raman Graphite/Disorder ratios (0.82-1.92-1.59-1.69-2.29), XPS atomic percent change (19% to 0%), filtration time (120 s per 50 ml contaminated solution per 0.5 g filter medium sample), and renewal time (180 s per 0.5 g filter medium sample) indicated that the first-of-its-kind filter is not only highly efficient, but also fully renewable.

II. TABLE OF CONTENTS

II. KEY WORDS

Chemical Vapor Deposition, Electronic Waste, Epoxidation, Functionalization, Heavy Metal Removal, Hydrochloric Acid Sonification, Multi-Walled Carbon Nanotubes, Nanotechnology, Water Filtration, Wet-Air Oxidation.

III. ABBREVIATIONS AND ACRONYMS

CVD: Chemical Vapor Deposition	SEM: Scanning Electron Microscopy
DCM: Dichloromethane	SENT: Supported Epoxidized Nanotube
G/D Ratio: Graphite to Disorder Ratio	SWNT: Single-Walled Carbon Nanotube
HCl: Hydrochloric Acid	UV-Vis: Ultraviolet-Visible Spectroscopy
m-CPBA: meta-Chlorperoxybenzoic Acid	WAO: Wet-Air Oxidation
MWNT: Multi-Walled Carbon Nanotube	XPS: X-Ray Photoelectron Spectroscopy

IV. ACKNOWLEDGEMENTS

I would like to sincerely thank Professor Andrew Barron of the department of Chemistry at Rice University for his guidance and for allowing me to conduct my research project in his lab and the Welch Foundation for financially supporting my work. Additionally, I would like to thank Dr. Alvin Orbaek, Dr. Enrico Andreoli, and Dr. Lauren Morrow for supervising me while I characterized samples and Ms. Jessica Heimann for helping me plan the purification and epoxidation stages. Finally, I would like to thank my parents and my high school science research teachers, Ms. Ashley Poloha and Mrs. Brenda Pinchbeck, for their constant encouragement and support throughout the duration of this project.

V. BIOGRAPHY

Perry is a 2015 graduate of Clear Lake High School in Houston, Texas, USA. He has been passionate about water purification ever since he entered high school and has been working on the creation of a renewable heavy metal filtration technology for the past three years; he is the lead author of a paper on this topic that is being submitted to the peer-reviewed journal *Nature Materials*. He is the 2014 Best of Category Winner in Environmental Sciences at the Intel International Science and Engineering Fair, a 2014 Gold Medalist at the International Sustainable World Project Olympiad, and has delivered a lecture on his research at Imperial College, London. He was his school's President of the National Science Honor Society, President of the Red Cross Club, Captain of the Foreign Extemporaneous Debate Team, and Vice-President of the Mu Alpha Theta Club. He will be attending Stanford University and hopes to make further significant contributions to science, technology, and society.

1. INTRODUCTION

1.1. Significance of Topic

Clean and abundant water is the keystone of thriving communities, but increasing demand and volatile climate patterns are depleting rivers and aquifers. Moreover, the quality of such water sources is threatened by noxious contaminants. Given the recent and significant rise of electronic waste and industrialization (Fig. 1), heavy metal pollutants such as mercury, lead, and cadmium are of particular concern (Huang, et al., 2014). Heavy metal exposure can cause severe health effects in humans, including decreased mental development, organ injury, nervous system impairment, cancer, and even death. These contaminants cannot be degraded, have the ability to dissolve in wastewaters, and can travel up the food chain through bioaccumulation. Moreover, heavy metals can also seep into groundwater, thereby contaminating drinking water sources. One of the most notable heavy metal disasters is the Minamata syndrome of the 1950s, in which sewage containing mercury from an industrial chemical plant in Japan leaked into water sources causing health complications for nearly 2 million people and over 1000 fatalities (McCurry, 2006).

Heavy Metal	Electronic Waste Sources	Industrial Waste Sources
Arsenic	LEDs, Transistors, Glass, Electronic Clocks & Watches.	Glass, Ore Smelting Byproducts, Algaecides, Cotton Harvesting Dessicant, Herbicides
Cadmium	Light-Sensitive Resistors, Paints, Batteries, Printer Inks and Toners.	Galvanized Pipes, Metal Refineries, Catalysts, Phosphate Fertilizers
Chromium	Pigments, Server Racks, Data Tapes.	Coolants, Engine Parts, Steel and Pulp Mills
Cobalt	Pigments, Magnets, Temperature Resistant Alloys.	Alloy Plants, Aircraft Engines, Grinding and Cutting Tools, Glass, Ceramics
Lead	Batteries, Cell Phone Coatings, Cathode Ray Tubes, Solder, Cables, CRTs.	Tire Wear, Lubricating Oil and Grease, Bearing Wear, Plumbing Systems, Bullets
Mercury	Batteries, Flat Screen Monitors, LCDs, Thermostats, Switches, Lamps.	Thermometers, Paper Industry, Chlorine and Caustic Soda Manufacturing, Dental Fillings
Nickel	Batteries, CDs/DVDs, Hard Disk, Capacitors, SIM Cards, Antennas, Microphones.	Gasoline, Lubricating Oil, Brake Emissions, Cigarettes, Catalysts
Zinc	Printed Circuit Boards, Solar Cells, Memory Devices, Varistors, Surge Protectors.	Tire Wear, Motor Oil, Grease, Brake Emisions, Corrosion of Galvenized Parts

Figure 1. Some Common Heavy Metals and their Sources of Pollution; Sources: Agency for Toxic Substances & Disease Registry and Environmental Protection Agency

Many contemporary technologies for heavy metal removal such as reverse osmosis, ion exchange, and phytoremediation have been developed; however, there is a still a significant need for a simple filtration technology that is regenerable, cost-effective, and readily serviceable. The most significant issue with current heavy metal filtration

technologies is that they are nonrenewable; thus once the filters are disposed of, the heavy metals they have absorbed are released back into the environment at an even higher concentration, thereby creating a cycle of contamination.

1.2. Background Information

Carbon has many allotropes – the most common ones are amorphous carbon, graphite, and diamond. The discovery of a carbon allotrope, named the carbon nanotube in 1991, was revolutionary from the perspectives of chemistry, physics and material science (Weisman and Subramoney, 2006). Carbon Nanotubes can be divided into two main categories: Single-Walled Carbon Nanotubes (SWNTs) and Multi-Walled Carbon Nanotubes (MWNTs). SWNTs are one atom thick and tens of atoms in circumference. MWNTs contain many single walled carbon nanotubes concentrically arranged and can span a few nanometers to about 100 nm in diameter. Carbon Nanotubes are uniquely poised for use in many applications such as water filtration due to their fibrous and mesoporous structure, high aspect ratio, and accessible external surface area (Upadhyayula et al., 2009).

Thin Film Deposition is the deposition of a layer of material ranging from fractions of a nanometer to several micrometers in thickness on a surface, or onto previously deposited layers. A thin film of nanotubes produced by Chemical Vapor Deposition (CVD) can be deposited on highly resilient, chemically inert, and porous surfaces such as quartz wool (Wang and Moriyama, 2011).

Functionalization is the introduction of functional groups to a surface. Carbon nanotube surfaces can be covalently (chemically) or non-covalently (physically) functionalized to achieve highly desirable surface properties. Epoxidation is one form of covalent functionalization that adds an epoxide group (a cyclic ether) to the surface carbons in MWNTs such that for every two carbon atoms there is one oxygen atom (Chattopadhyay et al., 2008; Ogrin et al., 2006). These oxygen atoms contain lone electron pairs, which makes them ideal Lewis-Bases, or electron pair donors. Furthermore, heavy metals tend to behave as Lewis-Acids, or electron pair acceptors, due to their empty p, d, or f-subshell orbitals (Leach et al., 2008). Since Lewis Acid-Base interactions facilitate the facile formation of chemical complexes upon rehybridization of the empty orbitals, epoxidized MWNTs have great potential for heavy metal adsorption (Zhao et al., 2011). Furthermore, these adsorbed heavy metals can also possibly be removed from the MWNTs without damaging the epoxide groups using a solution of dilute acetic acid, because decreasing the pH of the solution carbon is immersed in induces a positive external surface charge (from protons) on functional groups;

thus an electrostatic repulsion would be created between the functional epoxide groups and the positively charged heavy metal cations. This property of desorption could render the functionalized nanotubes renewable, and therefore, reusable.

2. MATERIALS AND METHODS

2.1. Overview

The investigation was divided into five stages, with samples taken at each stage for appropriate characterization. The characterization techniques utilized included: Raman Spectroscopy for determination of the purity of carbon nanomaterials; Scanning Electron Microscopy (SEM) for high-resolution images of nanotube growth patterns; Ultraviolet-Visible Spectroscopy (UV-Vis) for determination of the concentration of metal compounds in solution after filtration (Oliva-Chatelain and Barron, 2010); and X-Ray Photoelectron Spectroscopy (XPS) for determination of the chemical composition of the filter material after filtration and renewal (Zeng and Barron, 2010). The first three stages consisted of the preparation of the filter medium: the synthesis and deposition of carbon nanotubes on quartz wool, purification of the nanotubes, and their subsequent epoxide functionalization. Stage four involved the filtration of heavy metal compounds dissolved in de-ionized water; five metal compounds were tested: Cadmium Acetate Dihydrate [$Cd(CH_3COO)_2 \cdot 2H_2O$] , Lead Acetate Trihydrate [$Pb(CH_3COO)_2 \cdot 3H_2O$], Mercuric Chloride [$HgCl_2$], Nickel Nitrate Hexahydrate [$Ni(NO_3)_2 \cdot 6H_2O$], and Cobalt Chloride Hexahydrate [$CoCl_2 \cdot 6H_2O$]. Stage five involved renewing the filter medium after heavy metal filtration from stage four by treating it with de-ionized water and acetic acid. Stages four and five thus form a continuous cycle of filtration and renewal. Fig. 2 shows a flow diagram of the five-stage procedure and the characterization techniques employed at each stage.

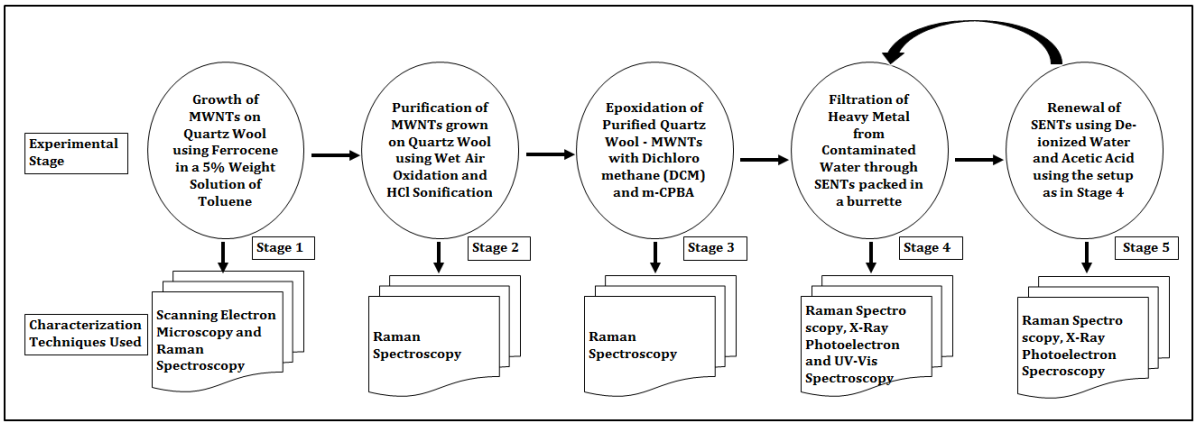

Figure 2. Five stages of the current investigation and the corresponding characterization techniques used.

2.2. Growth and Deposition of MWNTs on Quartz Wool (Stage 1)

In Stage 1, 4.33 g of ferrocene [$C_{10}H_{10}Fe$, 98%] were dissolved in 80 ml of toluene [C_7H_8, 99.8%] in a volumetric flask through bath ultrasonication, and then the flask was filled to the 100 ml mark to produce a 0.233 Molar solution. 3.45 g of 12 µm diameter quartz wool for nanotube deposition was placed in a 34 mm inner diameter x 38 mm outer diameter x 500 mm long quartz tube, which was then inserted into an SSP-354 Nanotech Innovations table-top growth furnace such that the quartz wool was positioned at the front of the growth zone (Orbaek et al., 2013). The instrument was calibrated as follows:

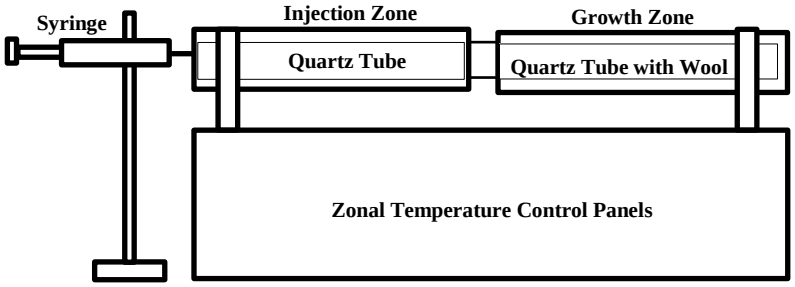

Figure 3. Surface deposition of carbon nanotubes on quartz wool using a Nanotech Innovations SSP-354 Furnace.

i) The inert gas flow regulator was set to 1.5 $L \cdot min^{-1}$ (5% Hydrogen, 95% Argon as obtained from Matheson Tri-Gas) and maintained for 25 min to remove any resident water vapor or other environmental impurities. Efficient ventilation of the exhaust gases was ensured.

ii) The injection and growth zone temperatures were set to 225°C and 900°C respectively.

Once the calibration was completed, 5 ml of the 5% by weight solution of ferrocene dissolved in toluene was transferred into a 6 ml syringe clamped in place by a Syringe Pump. The solution was injected into the tube furnace through a 9" injection needle obtained from Hamilton Syringe Company with the tip at middle of the injection zone at a rate of 3 ml/hr for 100 min (Fig. 3) along with the inert gas mixture previously used, and CVD was initiated to deposit the MWNTs on the quartz wool. Ferrocene serves as a catalyst under high temperatures and catalyzes the decomposition of toluene. Subsequently, it recombines the carbon within toluene to form

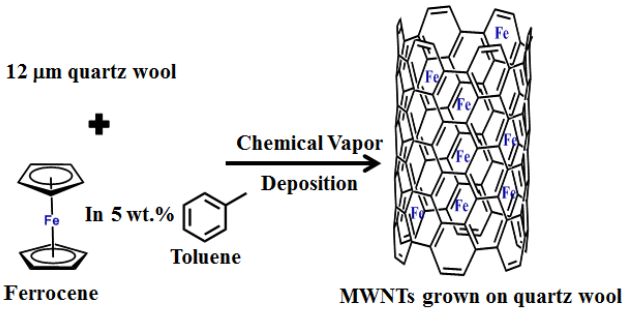

Figure 4. Stage 1 Reaction Mechanism: CVD of MWNTs on Quartz Wool with Toluene as the carbon source.

MWNTs on the surface of the quartz wool (Fig. 4). Both zones were cooled to 15°C after the full volume of the precursor solution was injected and the inert gas flow was turned off after a period of 50 min. The quartz tube was removed and cleansed in an acid bath (10% HCl) after extraction of the Quartz Wool-MWNTs.

2.3. Purification using Wet Air Oxidation and HCl Sonification (Stage 2)

Purification of the MWNTs was necessary before continuing to their epoxidation, because injection CVD is known to leave residual iron particles in the graphitic structure of the nanotubes. Before the purification process, two 5 mg samples of the MWNTs grown of Quartz Wool were extracted from the front and tail ends of the material for SEM and Raman Spectroscopy (633 nm incident laser wavelength) characterization. The material was then positioned at the front of the growth zone for purification. Wet-Air Oxidation (WAO) and Hydrochloric Acid (HCl) sonification were the two techniques utilized to effectively cleanse the nanotubes of residual impurities (Fig. 5). WAO oxidizes elemental iron impurities to Iron Oxide (Fe_2O_3), thereby providing hydrochloric acid the ability to permeate the nanotubes and leach out the iron particles, since Iron Oxide is soluble in HCl on the basis of polarity. An air source (approximately 78% Nitrogen and 22% Oxygen) was connected to a flow regulator set to a pressure of 1000 kPa, which was then connected to a bubbler filled 50% with de-ionized water. The bubbler, in turn, was connected to the reactor chamber inlet containing the Quartz Wool-MWNTs. WAO was initiated as the injection zone temperature regulator was set to 240°C and the growth zone temperature regulator was set to 37.5°C. The growth zone temperature was set to a relatively low value to minimize the risk of nanotubes burning off during the oxidation process. WAO was completed after 2 hours and 45 min; then, the Quartz Wool-MWNT material was placed in a beaker filled with 100 ml of 1M Hydrochloric acid and sonicated for 45 min in a Branson 3510-DTH Ultrasonic Cleaner. The contents of the beaker were then filtered through a 0.45 μm Polytetrafluoroethylene membrane and flushed with 1000 ml of water. The purified quartz wool MWNTs were placed in an oven and dried for 10 min.

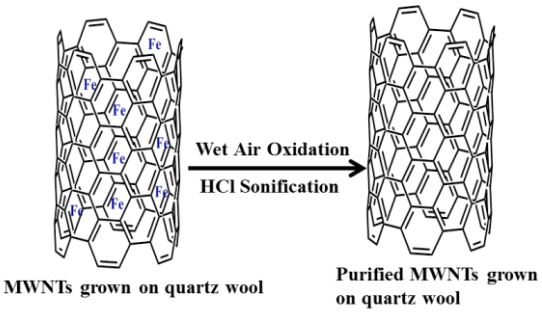

Figure 5. Stage 2 Reaction Mechanism: Purification of MWNTs through Wet Air Oxidation and HCl Sonification to remove iron and other impurities.

2.4. Functionalization with meta-Chlorperoxybenzoic Acid (m-CPBA) (Stage 3)

In Stage 3, the purified Quartz Wool-MWNTs were functionalized through epoxidation to form supported epoxidized nanotubes (SENTs) (Fig. 6). Before the epoxidation process, a 5 mg sample of the purified Quartz Wool-MWNT material was taken for analysis using Raman Spectroscopy (633 nm). Then, a 250 ml round bottom flask was filled with 200 ml of dichloromethane (DCM, CH_2Cl_2). 3.85 g of m-CPBA was then dissolved in the DCM by a magnetic stirrer for 10 min. The remaining purified Quartz Wool-MWNT material was then placed in this solution and stirred overnight with the same magnetic stirrer setup. The contents were poured through a 0.45 μm Polytetrafluoroethylene membrane, in vacuo, while being rinsed with 500 ml of DCM. The functionalization was complete after the SENT product was air dried in the back of a fume hood for 24 hours. The progression of the filter medium preparation is shown in Fig. 7.

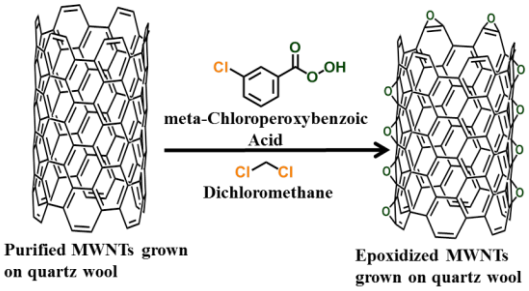

Figure 6. Stage 3 Reaction Mechanism: Epoxidation of MWNTs with m-CPBA dissolved in DCM to form Supported Epoxidized Nanotubes (SENTs).

Figure 7. Progression of Filter Medium Preparation Stages

2.5. Filtration of Heavy Metals using SENTs (Stage 4)

Filtration occurs through adsorption of a heavy metal compound by an epoxide group as shown in Fig. 8. Before the filtration process was initiated, a 5 mg sample of the material from stage 3 was removed for Raman analysis (633 nm). Calibration curves were then generated with five stock solutions of each metal compound dissolved in de-ionized water, prepared as follows: Cadmium Acetate Dihydrate- 0.02 M to 0.10 M in increments of 0.02 M; Mercuric Chloride- 0.002 M to 0.010 M in increments of 0.002 M; Nickel Nitrate

Hexahydrate- 0.002 M to 0.010 M in increments of 0.002 M; Cobalt Chloride Hexahydrate- 0.0002 M to 0.0010 M in increments of 0.0002 M; and Lead Acetate Trihydrate- 20 ppm to 100 ppm in increments of 20 ppm.

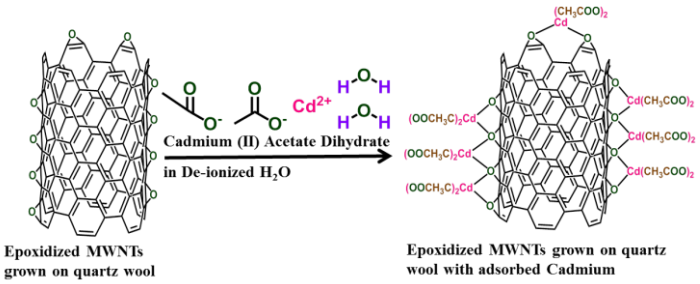

Figure 8. Stage 4 Reaction Mechanism: Filtration of Heavy Metal (Cadmium Acetate Dihydrate). The metal compound is adsorbed onto the SENTs- coordination occurs via the epoxide group.

Initially, a 0.052 M cadmium acetate dihydrate solution was prepared to simulate contaminated water by dissolving 1.8 g of cadmium acetate dihydrate in 150 ml of water. A 100 mL burette cleaned consecutively using a base bath with Potassium Hydroxide (KOH)/isopropyl alcohol, tap water, and de-ionized water was packed with 0.5 g of the SENTs. The burette was secured in a dual clamp setup (Fig. 9). 50 ml of the 0.052 M cadmium acetate dihydrate solution were then poured through the filter medium and an aliquot was collected at the bottom for UV-Vis analysis of filtration capacity. The filtration procedure was consecutively conducted two more times using the same filter medium with the same concentration and quantity of cadmium acetate dihydrate solution. The procedure was then repeated (with the appropriate changes in the stock solution preparation, a distinct filter medium sample, and three trials per metal to ensure repeatability) with a 0.01 M solution of Mercuric Chloride, 0.01 solution of Nickel Nitrate Hexahydrate, 1 millimolar solution of Cobalt Chloride Hexahydrate, and a 100 ppm solution of Lead Acetate Trihydrate. These particular concentrations were selected to simulate cases of high industrial wastewater and drinking water contamination. XPS was performed on the filter material following the first trial of cadmium filtration by selecting a small sample of the filter material after the filtration to probe for the presence of elemental cadmium. A time trial was conducted for each filtration trial to determine, on average, the speed of filtration in ml/min.

Figure 9. Filtration Setup.

2.6. Renewal of SENTs Filter Medium (Stage 5)

A 5 mg sample of the material was taken for Raman spectral analysis (633 nm) immediately after the cadmium filtration. For the renewal process, the filter material was treated with 50 ml of 50:50 (by volume) de-ionized water/acetic acid in the same burette after the three trials of cadmium filtration. The renewal process utilizes a 50:50 volumetric solution of de-ionized water and acetic acid to desorb metal compounds through electrostatic repulsion as shown in Fig. 10. A sample of the material after this procedure was taken for XPS analysis. Another time trial was conducted to determine how quickly the filter medium could be renewed. The resulting solution containing de-ionized water, acetic acid, and cadmium acetate was then collected below in a beaker, and subsequently left outside for 4 hours at an ambient temperature of 25°. The solution underwent natural evaporation to leave behind a caked residue of cadmium acetate. The effectiveness of the renewal procedure was then verified by conducting three additional consecutive filtration trials of cadmium acetate dihydrate, at the same concentration previously used, with the renewed filter medium.

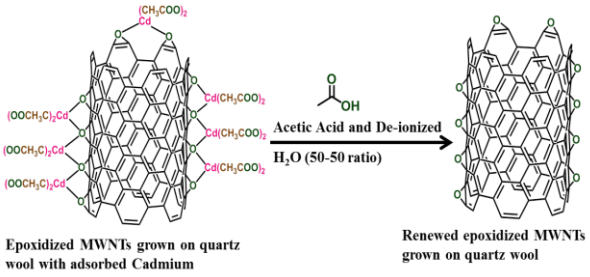

Figure 10. Stage 5 Reaction Mechanism: Renewal of SENTs Filter Using Acetic Acid and De-ionized Water by electrostatic repulsion between the epoxide group and heavy metal cation.

2.7. Saturation Trials

In order to determine the maximum quantity of contaminated water the filter medium could purify before renewal was necessary, saturation trials were conducted. 50 ml of a 100 ppm solution of Lead Acetate Trihydrate was poured through 0.5 g of a freshly prepared filter medium and the aliquot was collected at the bottom for UV-Vis analysis to determine filtration capacity. Following the filtration, the filter medium was rinsed with de-ionized water to desorb any physically absorbed lead and the resulting solution was stored separately from the aliquot. This filtration procedure followed by rinsing with de-ionized water was consecutively conducted twelve times using the same filter medium. Eluent analysis using UV-Vis was performed after each aliquot was collected to determine the changes in the filtration capacities as the trials progressed. The results of the saturation trials were then analyzed to determine the maximum volume of contaminated water the medium could purify with greater than 99% filtration capacity.

3. RESULTS AND DISCUSSION

3.1. Growth and Purification

The MWNT deposition took place in the Nanotech Innovations Furnace, which utilized CVD to deposit MWNTs on Quartz Wool. For the 3.45 grams of quartz wool used, 10 grams of MWNTs were produced through CVD. The growth process indicated that the deposition density on the quartz wool was uniform and the wool was "visually dark" throughout its length. This uniformity is important, because non-linear deposition would only allow for a small sample of the Quartz Wool-MWNT Material to be used, which would render the CVD growth process inefficient.

The WAO process demonstrated no perceptible change in the appearance of the carbon nanotubes, although the filter medium had a greater mass after the process, as expected due to additional oxygen atoms from oxidation. Following the HCl sonification of the MWNTs, a distinct yellow color was visible in the solution collected after the purified filter medium was flushed with water, indicating purification (Fe^{3+} ions produce a yellow hue in solution).

3.2. SEM Images

SEM images of the front end and the tail end sections of the Quartz Wool- MWNT material were taken to examine how the MWNTs were deposited on quartz wool fibers. SEM characterization was carried out with FEI Quanta 400 by placing samples on double-sided carbon tape that was fixed to aluminum SEM stubs. Images were acquired at a typical operating voltage of 20 kV, with a working distance of 10 mm, spot size 3 in Hi-VAC mode.

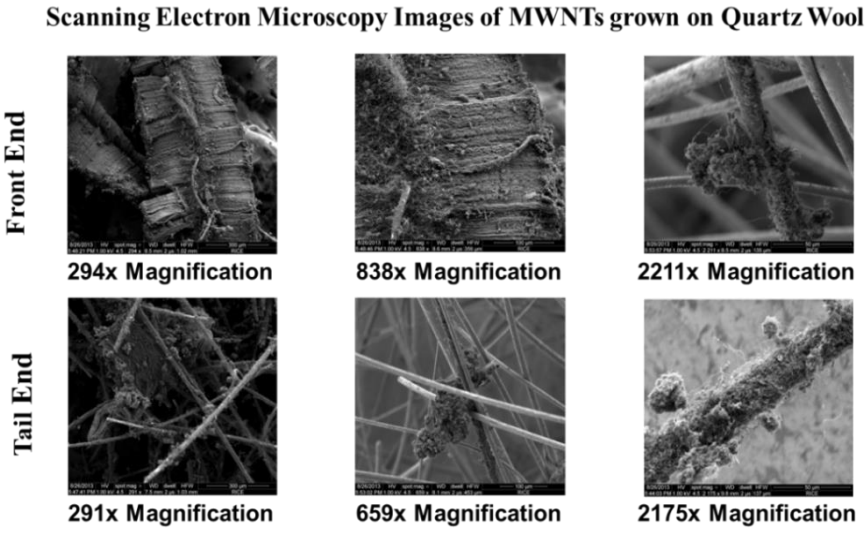

Figure 11. Scanning Electron Microscopy (SEM) Images of the front and tail ends of MWNTs grown on quartz wool.

Over 50 images were generated from both samples with magnifications ranging from x94 to x3664. Fig. 11 shows selected views of samples from the front and tail end of the filter medium for comparison. The images indicated that the deposition was uniform, with the front and tail ends of the wool displaying ample growth of MWNTs. Higher magnification (3430x and 3664x) clearly showed deposition of nanotubes in both ends. Additionally, SEM analysis demonstrated that many nanotubes had a length of over 20 microns.

3.3. Filtration and UV-Vis Spectroscopy

Calibration curves for each heavy metal compound were generated to determine the filtration capacity of the filter medium. Initially, absorbance spectra were generated for 5 stock solutions for each of the 5 metal compounds, for a total of 25 spectra. Then, the wavelength at which each spectrum had a maximum absorbance was taken, with each metal compound having a particular peak wavelength. The UV-Vis Peak absorbance wavelengths were 199 nm for Cd (Fig. 12 and Fig. 13), 485 nm for Hg (Fig. 14 and Fig. 15), 301 nm for Ni (Fig. 16 and Fig. 17), 485 nm for Co (Fig. 18 and Fig. 19), and 655 nm for Pb (Fig. 20 and Fig. 21). The peak absorbance values at the respective peak wavelengths for each metal compound were plotted against the stock solution concentrations such that the absorbance values had a linear relationship (least squares regression) with the standard molar concentrations used. Upon the completion of the calibration curves, absorbance spectra were generated for each of the aliquots (solution collected below the burette after filtration of the heavy metal) for a total of 15 spectra. The peak absorbance value of each of these spectra was located using the peak wavelengths determined from the stock solution spectra. Given the peak absorbance value of each of the spectra, the concentration of the aliquot could be determined using linear interpolation. Once the concentration was determined, the filtration capacity of the filter medium for each heavy metal compound was computed as follows:

$$Filtration\ Capacity = \left[1 - \frac{Concentration\ of\ Filtered\ Solution}{Initial\ Concentration}\right] \times 100\%$$

The interpolation of the average peak absorbances yielded post-filtration heavy metal concentrations with three-trial average filtration capacities of 99.39% for Cadmium, 99.61% for Mercury, 99.70% for Nickel, 99.72% for Cobalt, and 99.97% for Lead (Table 1). Thus, for example, heavy metal-contaminated sources as high as 750 μg/L can be filtered to meet the current Environmental Protection Agency Maximum Contaminant Level Goal of 1 μg/L. However, even in extreme cases, heavy metal levels have not been found to exceed 100 μg/L in worldwide water sources (Meybeck et al., 1989).

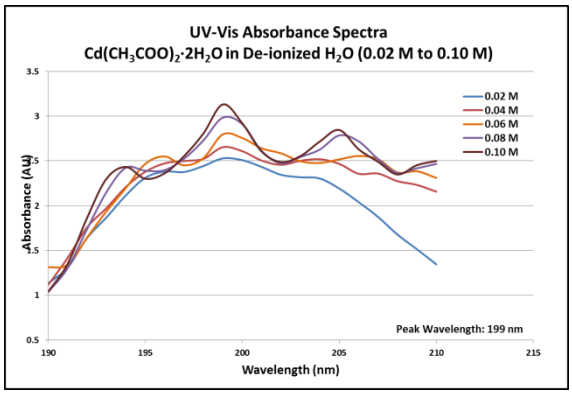

Figure 12. UV-Vis Absorbance Spectra of Cadmium Acetate Dihydrate: The spectra for molar concentrations of 0.02M - 0.10M were used to generate the calibration curve at a peak absorbance wavelength of 199 nm.

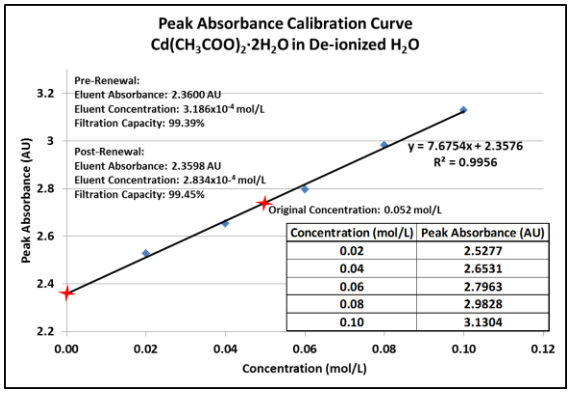

Figure 13. UV-Vis Calibration Curve for Cadmium Acetate Dihydrate: Linear mathematical relationship between Concentration and Peak Absorbance at the peak absorbance wavelength of 199 nm.

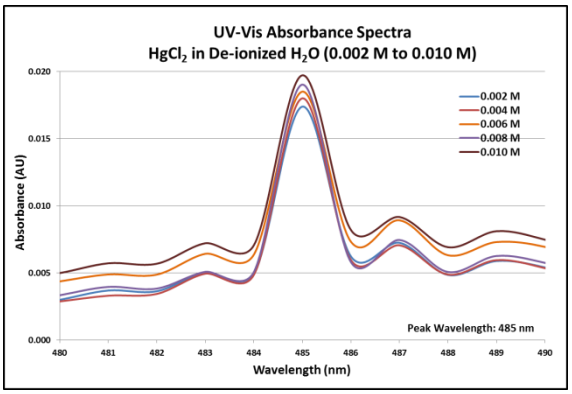

Figure 14. UV-Vis Absorbance Spectra of Mercuric Chloride: The spectra for molar concentrations of 0.002M - 0.010M were used to generate the calibration curve at the peak absorbance wavelength of 485 nm.

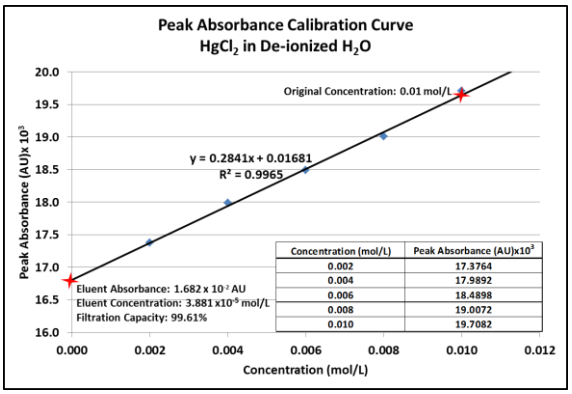

Figure 15. UV-Vis Calibration Curve for Mercuric Chloride: Linear mathematical relationship between Concentration and Peak Absorbance at the peak absorbance wavelength of 485 nm.

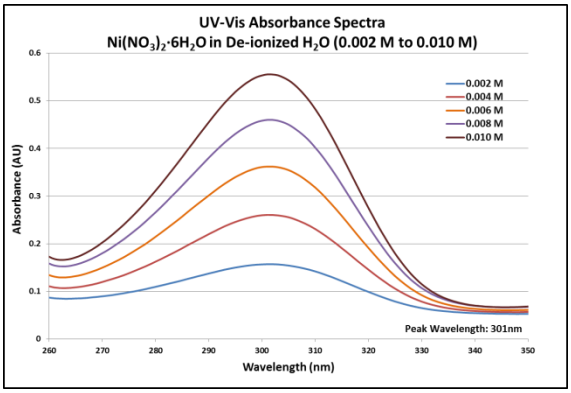

Figure 16. UV-Vis Absorbance Spectra of Nickel Nitrate Hexahydrate: The spectra for molar concentrations of 0.002M - 0.010M were used to generate the calibration curve at the peak absorbance wavelength of 301 nm.

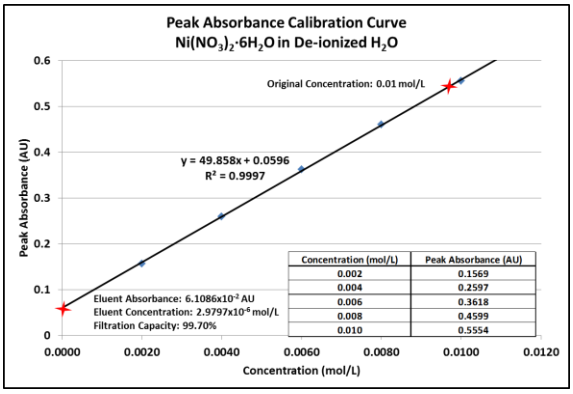

Figure 17. UV-Vis Calibration Curve for Nickel Nitrate Hexahydrate: Linear mathematical relationship between Concentration and Peak Absorbance at the peak absorbance wavelength of 301 nm.

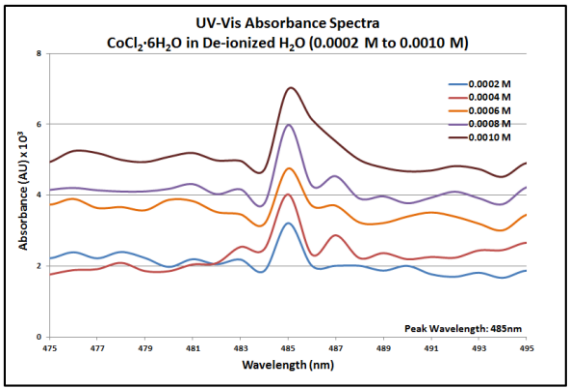

Figure 18. UV-Vis Absorbance Spectra of Cobalt Chloride Hexahydrate: The spectra for molar concentrations of 0.0002M - 0.0010M were used to generate the calibration curve at the peak absorbance wavelength of 485 nm.

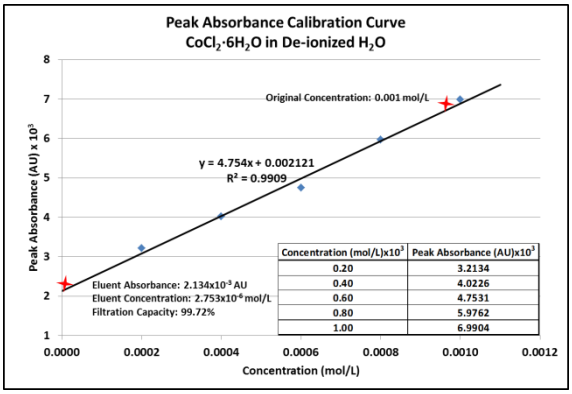

Figure 19. UV-Vis Calibration Curve for Cobalt Chloride Hexahydrate: Linear mathematical relationship between Concentration and Peak Absorbance at the peak absorbance wavelength of 485 nm.

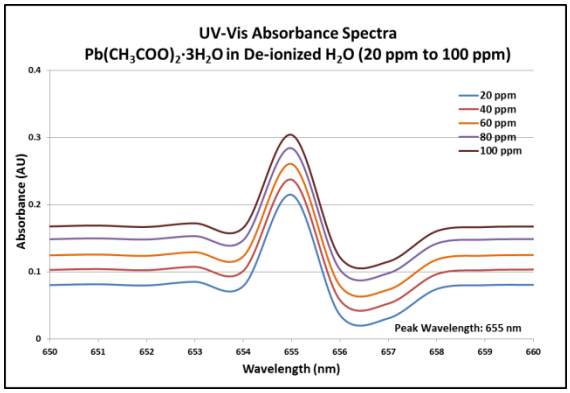

Figure 20. UV-Vis Absorbance Spectra of Lead Acetate Trihydrate: The spectra for molar concentrations of 20 ppm – 100 ppm were used to generate the calibration curve at the peak absorbance wavelength of 655 nm.

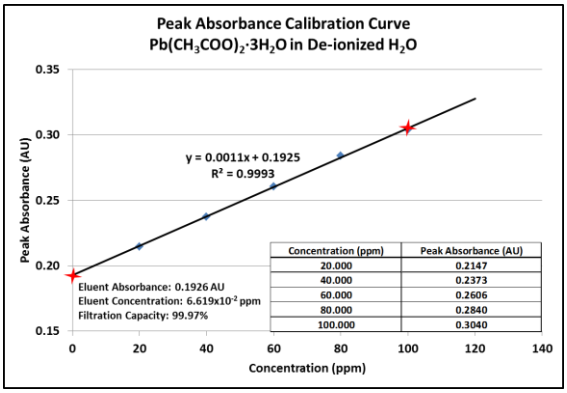

Figure 21. UV-Vis Calibration Curve for Lead Acetate Trihydrate: Linear mathematical relationship between Concentration and Peak Absorbance at the peak absorbance wavelength of 655 nm.

Metal Contaminant	Absorbance (AU)	Concentration (mol/L)	Filtration Capacity (%)
Cadmium	2.3600	3.1861E-04	**99.3873**
Mercury	0.0168	3.8807E-05	**99.6119**
Nickel	0.0611	2.9797E-05	**99.7020**
Cobalt	0.0021	2.7529E-06	**99.7247**
Lead	0.1926	1.4396E-07	**99.9702**

Table 1. Three-Trial Average Filtration Capacities for various Metal Compounds: The absorbance represents the average peak absorbance value obtained through UV-Vis analysis for each metal compound; concentration refers to the average quantity of dissolved metal remaining after filtration as determined through linear interpolation of calibration curves; filtration capacity represents how much contaminated water the filter medium can purify.

3.4. XPS Spectra

XPS spectra were acquired on a PHI 5700 ESCA system (Physical Electronics) at 15 kV, using an aluminum target and an 800 μm aperture; samples were pressed into indium metal. The XPS spectra obtained after the filtration of Cadmium showed that 19% of the atoms within the filter medium were cadmium atoms, while 42.7% of the atoms were carbon atoms and 38.3% of the atoms were oxygen atoms (Fig. 22). This discovery demonstrates that the filter medium adsorbed a significant amount of cadmium during the filtration process. Hence, it corroborates the findings determined using UV-Vis. However, after the filter medium was rinsed with de-ionized water and acetic acid, the cadmium atomic % dropped to zero, and the composition of the filter material was 76.7% carbon and 23.3% oxygen (Fig. 23); thus the filter medium can be reused for filtration again.

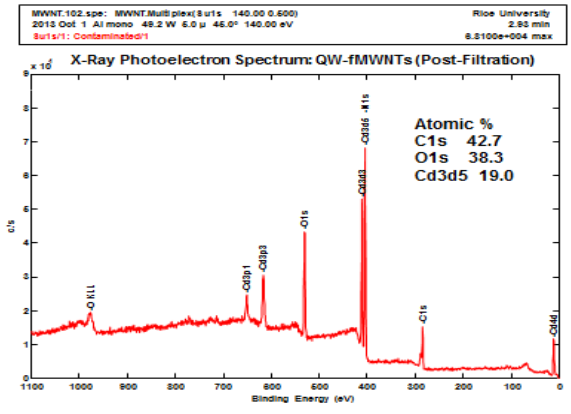

Figure 22. XPS after filtration: The spectrum shows that 19% of the atoms in the post-filtration material were composed of cadmium.

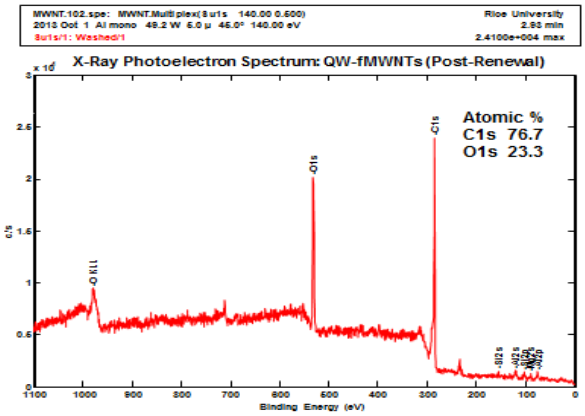

Figure 23. XPS after filter regeneration: The spectrum illustrates that 0% of the atoms in the post-renewal material were composed of cadmium.

Furthermore, a detailed material balance calculation of the atomic percentages of oxygen before and after regeneration showed that there was a negligible loss of epoxide groups during the renewal process, ensuring recyclability. The theoretical and experimental percentages of carbon and oxygen after the renewal process were compared: according to the calculation, there should have theoretically been 76.4% Carbon and 23.6% Oxygen assuming all of the cadmium acetate was desorbed, while the experimental results were remarkably consistent, with 76.7% Carbon and 23.3% Oxygen.

3.5. Raman Spectra

Raman spectroscopy was utilized to analyze the changes in the purity of the nanotubes as the stages progressed. Spectra were obtained using a Renishaw inVia Raman

Microscope, at a 633 nm wavelength, using a 50x Long Working Distance lens; data was acquired with 3 accumulations between 100 cm^{-1} and 3300 cm^{-1} with cosmic-ray background removal applied. Since the G′ peak was the most prominent of spectral peaks, it was used to calibrate the laser spot to maximize signal intensity at the detector. For Stages 4 and 5, only the filter medium samples after the filtration of Cadmium Acetate Dihydrate and the subsequent renewal were used. The purity of the nanotubes could be assessed by the G-Peak to D-Peak Ratio. The Graphite-Peak is indicative of sp^2 hybridized carbon, while the Disorder-Peak is indicative of sp^3 hybridized carbon. Since nanotubes follow sp^2 hybridization, the higher the Graphite-to-Disorder (G/D) Ratio, the more pure the nanotubes are. After Raman spectra were produced for the five stages, the G-Peak was normalized at an intensity of 1.00 to simplify the direct comparison of G/D ratios as shown in Fig. 24.

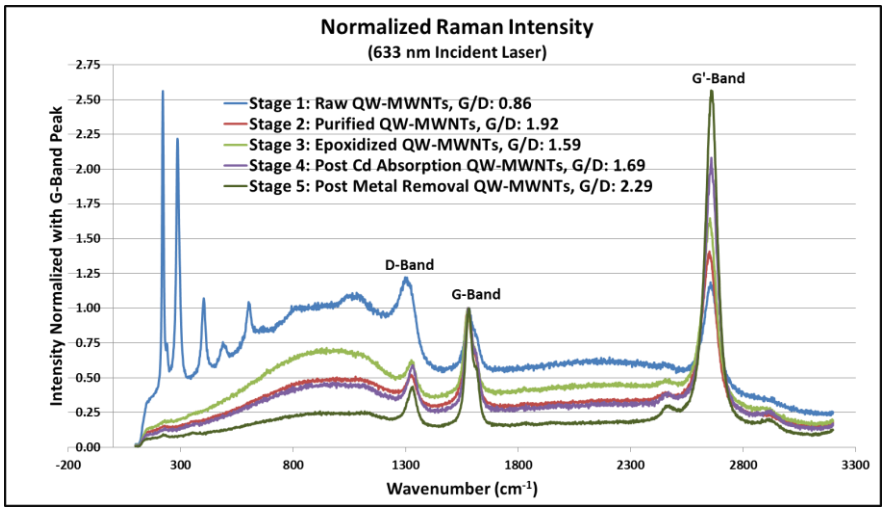

Figure 24. Raman intensities during the five stages of the current investigation: The spectra were normalized with the G-Peak (wavenumber of 1600 cm^{-1}). Successive G/D or purity ratios illustrate the changes in the purity of the nanotubes as the stages of the investigation progressed.

After the purification process, the G/D ratio increased from 0.86 to 1.92, which illustrated that the purity of the MWNTs was significantly enhanced due to the removal of iron impurities. Analysis after epoxidation showed a slight decrease in the G/D ratio to 1.59 from 1.92, which was expected, because the addition of the epoxide groups to MWNTs slightly disrupts the graphitic structure of the nanotubes. There was an insignificant change in the ratio after filtration of Cadmium (Stage 4), which was also anticipated, because the graphitic structure of the nanotubes does not undergo any change after the filtration with cadmium; the epoxide group alone is responsible for adsorbing heavy metal compounds. However, the G/D ratio increased significantly to 2.29 after renewal, which indicates that the graphitic structure

was not only restored completely through regeneration, but also that some of the other impurities such as iron, amorphous carbon, and graphite may have been stabilized.

3.6. Regeneration, Time Trials, and Saturation Trials

The renewal procedure devised allows for metals to be extracted from the filter medium for productive use with only natural evaporation. The resulting solution after the renewal process containing de-ionized water, acetic acid, and cadmium acetate was allowed to fully evaporate for four hours. The de-ionized water and acetic acid vaporized, leaving behind a caked residue of pure cadmium acetate.

After the renewal of the filter medium that was used for the filtration of cadmium acetate, three additional filtration trials with cadmium acetate of the same concentration and quantity as before on the renewed medium demonstrated that the filtration capacity remained high at 99.45%. A Two-Sample T-Test conducted to compare the filtration capacity of the filter medium before and after the renewal demonstrated the sustainability of the filter medium.

Saturation trials conducted with 100 ppm Lead Acetate Trihydrate indicated that the filtration capacity remained greater than 99.9% for 7 consecutive filtrations of 50 ml each, and then quickly deteriorated to 55.5% within the next 5 trials (Table 2) indicating saturation. Thus 350 ml of the solution was filtered successfully by 0.5 g of the SENTs filtration medium, after which regeneration was necessary.

DI-Pb Trial #	Absorbance (AU)	Calculated Concentration (ppm)	Filtration Capacity %
1	0.1926	3.17E-02	**99.9683**
2	0.1926	1.69E-02	**99.9831**
3	0.1926	2.89E-02	**99.9711**
4	0.1926	2.88E-02	**99.9712**
5	0.1926	4.87E-02	**99.9513**
6	0.1926	7.80E-02	**99.9220**
7	0.1926	9.04E-02	**99.9096**
8	0.1941	1.44E+00	**98.5568**
9	0.2014	8.04E+00	**91.9615**
10	0.2107	1.65E+01	**83.4559**
11	0.2255	2.99E+01	**70.0595**
12	0.2415	4.45E+01	**55.5298**

Table 2. Lead Saturation Trials: The absorbances represent the peak absorbance values obtained through UV-Vis analysis of the eluents in the 12 consecutive filtrations, 50 ml at a time, of 100 ppm Lead Acetate Trihydrate solution. A calibration curve was used to determine each of the respective calculated concentrations. The filtration capacity stayed at a value > 99.9% through 7 consecutive trials (for a total of 350 ml) and then rapidly decreased to 55.5% within the next 5 trials, indicating saturation, and thus providing a measure of overall filtration capacity.

Time trials for the filtration process demonstrated that the filter medium, on average, took 120 seconds to filter 50 ml of contaminated water, while the renewal process took approximately 180 seconds to complete. For a scaled-up version of the filter medium suitable for domestic settings (200x the sample used in the experiment), the filter material can thus filter 5 L of water in 1 minute and be renewed in just 1.5 min.

4. CONCLUSIONS

4.1. General Findings

A uniform deposition of MWNTs on quartz wool was successfully accomplished through use of CVD followed by purification and functionalization. Additionally, the simple assembly of the filter medium and the recent advances in inexpensive nanotube production make it suitable for both domestic and industrial settings. All heavy metals used were effectively filtered from the contaminated water solution by the SENTs medium, as evidenced through UV-Vis analysis. The high porosity of quartz wool and its low density packing ensured that the resistance to flow was minimal, thus making the filtration quick and effective.

The 3-trial average of UV-Vis analysis indicated filtration capacities of 99.39% for Cadmium, 99.61% for Mercury, 99.70% for Nickel, 99.72% for Cobalt, and 99.97% for Lead. Overall, it is very promising that the filter medium was remarkably successful and could absorb well over 99% of five distinct heavy metal contaminants at significantly high concentrations. Time trials indicated that a scaled-up version of the filter (200x) could filter 5 L of water in 1 minute and be renewed in just 1.5 min; moreover, the 12-trial lead saturation analysis indicated that the filter could maintain a filtration capacity greater than 99.9% for up to 70 L / 100 g of the SENTs filter medium, before it needed to be renewed.

The heavy metal compounds from the filter medium were successfully removed using de-ionized water and acetic acid, as evidenced from XPS spectra and the epoxide group material balance. This shows promise for recycling the filter for repeated use. Subsequent filtration after the renewal also showed that the filter medium is consistent (99.39% filtration capacity before renewal v. 99.45% filtration capacity after renewal). Moreover, the renewal process devised introduces the added benefit of allowing the metals to be extracted from the filter medium for further reuse in industrial applications.

4.2. Future Work

One possible extension is to vary the functionalization mechanisms on the MWNTs to allow for removal of other water contaminants in various solvents. For example, amino functionalized MWNTs can be used to remove mercury ions from fish oil and antimicrobial polymer functionalized MWNTs can be used to remove bacteria and microorganisms from water (Soleimani et al., 2014). Varying the type of functionalization on the filter medium can greatly increase its versatility and applicability in a variety of industries. One starting point that may elucidate this possibility is conducting Energy-dispersive X-ray spectroscopy on the SENTs material and creating an elemental analysis map to confirm the MWNT coordination environment and the presence of adsorbed anions in the material.

Finally, material costs can be further minimized by optimally varying the volume of SENTs used for filtration or the base material used for the filter medium (e.g. Glass Wool instead of Quartz Wool).

5. REFERENCES

Chattopadhyay, Jayanta, Amab Mukherjee, Christoper E. Hamilton, JungHo Kang, Soma Chakraborty, Wenhua Guo, Kevin F. Kelly, Andrew R. Barron, and W. Edward Billups (2008) "Graphite Epoxide." [Online] *Journal of the American Chemical Society*. [Online] 120 (16). p.5414-5415. Available from: http://pubs.acs.org/doi/abs/10.1021/ja711063f. [Accessed: 23rd October 2013].

Huang, J., Nkrumah, P., Anim, D., & Mensah, E. (2014) "E-Waste Disposal Effects on the Aquatic Environment: Accra, Ghana." *Reviews of Environmental Contamination and Toxicology* 229. p.19-34.

Leach, Mark. (2008) "Lewis Acid/Base Interaction Matrix Database." *The Chemogenesis Web Book*. [Online] Available from: http://www.meta-synthesis.com/webbook/13_lab-matrix/matrix.php?id=1338. [Accessed: 10th December 2013].

McCurry, J. (2006) Japan remembers Minamata. *Lancet* 367 (9505) p.99-100.

Meybeck, M., Chapman, D.V. and Helmer, R. (1989) Global Freshwater Quality: A first assessment, *GEMS Global Environment Monitoring System*, WHO/UNEP, Blackwell, Oxford.

Ogrin, Douglas, Jayanta Chattopadhyay, Anil K. Sadana, W. Edward Billups, and Andrew R. Barron. (2006) "Epoxidation and Deoxygenation of single-walled carbon nanotubes:

quantification of epoxide defects." *Journal of the American Chemical Society*. [Online] 128 (35) p.11322-11323. Available from: http://pubs.acs.org/doi/abs/10.1021/ja061680u.

Oliva-Chatelain, Brittany L., and Andrew R. Barron. (2010) "Basics of UV-Visible Spectroscopy." *Connexions Project*. m34525. Available from: http://cnx.org/contents/02e7b3d6-cf47-4c92-a380-d011ce5658b1@1. [Accessed: 27th October 2013].

Orbaek, Alvin W., Neerja Aggarwal, and Andrew R. Barron. (2013) "The development of a 'process map' for the growth of carbon nanomaterials from ferrocene by injection CVD." *Carbon*. Submitted.

Soleimani, Majid, Majid G. Afshar, and Arman Sedghi. (2013) "Amino-Functionalization of Multiwall Carbon Nanotubes and Its Use for Solid Phase Extraction of Mercury Ions from Fish Sample." *ISRN Nanotechnology*. [Online] Article 674289. Available from: http://www.hindawi.com/isrn/nanotechnology/2013/674289/. Accessed: [19th January 2014].

Upadhyayula, Venkata K.K., Shuguang Deng, Martha C. Mitchell, and Geoffrey B. Smith. (2009) "Application of carbon nanotube technology for removal of contaminants in drinking water: A review." *Science of the Total Environment* 408 p.1-13.

Wang, Qiguan and Moriyama, Hiroshi, (2011) "Carbon Nanotube-Based Thin Films: Synthesis and Properties", in Yellampalli, Siva (ed.) Carbon Nanotubes - Synthesis, Characterization, Applications. : INTECH Open Access, pp. 487-514. Available from: http://cdn.intechopen.com/pdfs-wm/16817.pdf [Accessed: 19th October 2013].

Weisman, Bruce, and Shekhar Subramoney. (2006) "Carbon Nanotubes." *Electrochemical Society Interface* p.42-46.

Zeng, Liling, and Andrew R. Barron. (2010) "Characterization of Covalently Functionalized Single-Walled Carbon Nanotubes." *Connexions Project*. m22299. Available from: http://cnx.org/contents/32119e66-825d-4320-a631-cb9c9ea96ba2@4. [Accessed: 27th October 2013]

Zhao, Guixia, Jiaxing Li, Xuemei Ren, Changlun Chen, and Xiangke Wang. (2011)"Few-Layered Graphene Oxide Nanosheets As Superior Sorbents for Heavy Metal Ion Pollution Management." *Journal of the American Chemical Society*. [Online] 45 (24) p.10454–10462. Available from: http://pubs.acs.org/doi/abs/10.1021/es203439v. [Accessed: 23th October 2013]